

**COMPARISON BETWEEN HYDROSTATIC AND NONHYDROSTATIC
SIMULATIONS OF TURKISH STRAIT SYSTEM**



M.Sc. THESIS

Ece Nil Parkan

Department of Solid Earth Sciences

Geodynamics Programme

DECEMBER 2018

ISTANBUL TECHNICAL UNIVERSITY ★ EURASIA INSTITUTE OF EARTH SCIENCES

**COMPARISON BETWEEN HYDROSTATIC AND NONHYDROSTATIC
SIMULATIONS OF TURKISH STRAIT SYSTEM**



M.Sc. THESIS

**Ece Nil Parkan
(602161002)**

Department of Solid Earth Sciences

Geodynamics Programme

Thesis Advisor: Assoc. Prof. Dr. Mehmet ILICAK

DECEMBER 2018

İSTANBUL TEKNİK ÜNİVERSİTESİ ★ AVRASYA YER BİLİMLERİ ENSTİTÜSÜ

**HİDROSTATİK VE HİDROSTATİK OLMAYAN TÜRK BOĞAZLAR
SİSTEMİ SİMÜLASYONLARININ KARŞILAŞTIRILMASI**

YÜKSEK LİSANS TEZİ

**Ece Nil Parkan
(602161002)**

Katı Yer Bilimleri Anabilim Dalı

Jeodinamik Programı

Tez Danışmanı: Doç. Dr. Mehmet ILİCAK

ARALIK 2018

Ece Nil PARKAN, a M.Sc. student of ITU Eurasia Institute of Earth Sciences student ID 602161002, successfully defended the thesis/dissertation entitled “COMPARISON BETWEEN HYDROSTATIC AND NONHYDROSTATIC SIMULATIONS OF TURKISH STRAIT SYSTEM”, which she prepared after fulfilling the requirements specified in the associated legislations, before the jury whose signatures are below.

Thesis Advisor : **Assoc. Prof. Dr. Mehmet ILICAK**

Istanbul Technical University

Jury Members : **Assoc. Prof. Dr. Ufuk Utku TURUNÇOĞLU**

Istanbul Technical University

Assoc. Prof. Dr. Emre OTAY

Bogazici University

Date of Submission : 16 November 2018

Date of Defense : 13 December 2018





To my family, my friends and my partner



FOREWORD

Although it was hard for me at first to study in this area, in time, curiosity took me somewhere else in this field and made me to drive learning for more. Thus, I appreciate my advisor for his efforts and understanding of this challenging situation that force us to succeed our work in a limited of time. I also grateful to my friend Alican PEKİYİ and Dr. Can ÜLKER for their supports and believing in me to succeed.

November 2018

Ece Nil Parkan
(Geophysical Engineer)



TABLE OF CONTENTS

	<u>Page</u>
FOREWORD	ix
TABLE OF CONTENTS	ixi
ABBREVIATIONS	xiii
SYMBOLS	xv
LIST OF TABLES	xvii
LIST OF FIGURES	xix
SUMMARY	xxi
ÖZET	xxiii
1. INTRODUCTION	1
2. LITERATURE REVIEW	3
3. GOVERNING EQUATIONS	5
3.1. Introduction	5
3.2. Mathematical Formulations.....	5
3.2.1. Basic equations.....	5
3.2.2. Boussinseq approximation	7
3.2.3. Hydrostatic approximation	8
4. MODEL CONFIGURATION OF THE NUMERICAL MODEL	11
5. INTERPRETATIONS AND RESULTS	15
5.1. Numerical Model Results with Hydrostatic Solution	15
5.1.1. Temperature and salinity distribution along the Dardanalle Strait	15
5.1.2. Temperature and salinity distribution along the Bosphorus Strait.....	16
5.1.3. Temperature and salinity distribution along the TSS.....	18
5.1.4. Sea surface height and vorticity of the Marmara Sea.....	19
5.2. Comparison of Hydrostatic Simulation with Non-Hydrostatic Simulation	20
5.2.1. Temperature and salinity distribution along the Dardanelle Strait	20
5.2.2. Temperature and salinity distribution along the Bosphorus Strait.....	21
5.2.3. Temperature and salinity distribution along the TSS.....	22
5.2.4. Sea surface height and vorticity of the Marmara Sea.....	24
6. CONCLUSIONS	27
7. FUTURE STUDIES	29
REFERENCES	31
CURRICULUM VITAE	35



ABBREVIATIONS

S	: Salinity
T	: Temperature
TSS	: Turkish Strait System
BS	: Bosphrous Strait
DS	: Dardanelle Strait
M	: Marmara Sea
SSS	: Sea Surface Salinity
SST	: Sea Surface Temperature
SSH	: Sea Surface Height
CIL	: Cold Intermediate Layer



SYMBOLS

k_s	: Salt Diffusion
k_T	: Thermal Conductivity
C_v	: Heat Capacity
t	: Time
u, v, w	: Velocity Vector Components
ρ	: Density





LIST OF TABLES

	<u>Page</u>
Table 4.1: Model parameters used in TSS	14





LIST OF FIGURES

	<u>Page</u>
Figure 1.1 : Bathymetry map of the Marmara. Solid lines show: red for along the whole Thalweg line, cyan colored line (26.1806E 40.0328N -26.7199E 40.4193N) for DS and green one (28.9999E 41.0232N-29.1394E 41.2345N) for BS.	2
Figure 3.1 : Illustration of bottom and surface boundary notation. Moving surface is impermeable while $z=\eta$ in 3.15, taken from Cushman Roisin et al. (2011)	9
Figure 4.1 : Model grid domain of the study area.	12
Figure 4.2 : Grid spacing in the x-direction (dx) of model domain	13
Figure 4.3 : Grid spacing in the y-direction (dy) of model domain.	13
Figure 5.1 : Time averaged section (A) for Temperature and (B) for Salinity between two chosen coordinates in Figure 1.2 along thalweg line for Dardanelle with no barotropic volume flux. Black lines show contours and the numbers on them show their values.	16
Figure 5.2 : Temperature section(A) and Salt section(B) between two chosen coordinates in Figure 1.2 along thalweg line for Bosphrous Strait with no barotropic volume flux	17
Figure 5.3 : Sections of Salinity (B,D) and Temperature (A,C) along Thalweg line which includes starting from Mediterrenean sea, Dardanelle Strait, Marmara Sea and Bosphrous Strait to come an end in the Black sea respectively.	18
Figure 5.4 : The mean sea surface height field.	19
Figure 5.5 : The mean relative vorticity normalized by the Coriolis force.	20
Figure 5.6 : Temperature section (A) and Salt section (B) difference of Dardanelle along thalweg with no flux.	21
Figure 5.7 : Temperature section (A) and Salt section (B) difference of Bosphorus along thalweg with no flux.	22
Figure 5.8 : Sections of difference for Salinity (B,D) and Temperature (A,C) along Thalweg line.	23
Figure 5.9 : Change Sea Surface Height Difference in the Marmara under the coupling behavior of Strait System.	25
Figure 5.10 : Sea surface vorticity difference between two simulations.	25



COMPARISON BETWEEN HYDROSTATIC AND NONHYDROSTATIC SIMULATIONS OF TURKISH STRAIT SYSTEM

SUMMARY

Turkish Strait System (TSS) consists of Dardanelle Strait, Marmara Sea and Bosphorus Strait is a coupled system where the fully coupled effects are significantly different than three individual members of the system. Due to the deep inflow from Mediterranean Sea and also outflow of the Black Sea, Marmara Sea acts like a buffer zone of these two important water masses. In addition, the Marmara Sea has its own separate temperature and salinity water characteristics that is resulted in significantly different stratified layers than the neighbor seas.

The more saline (38 psu) and warmer (26°C) waters from the Mediterranean Sea mixes with colder (22°C) and less saline (18 psu) Black Sea water in the Marmara Sea and creates cold intermediate layer (CIL) which is highly effected from surface fluxes that will change its thickness and depth from the surface. We employ a 3D hydrostatic and non-hydrostatic ocean general circulation model in this study. The hydrostatic simulation is carried out from Sanino et al, 2017, where they investigate the impact of volume fluxes on the TSS circulation. The initial conditions for the three different Seas are based on the measurements that are taken from the CTD's during the summer season. This initalized warm upper surface waters along basins, couldn't reach to climatological cold surface water of Black Sea without heat fluxes like in the other months of the year. Surface waters, summer time is the special case, are colder in general. (According to the SHOD(2009), Month of February Dardanelle Strait has temperature down to 8.6°C; and in the Bosporus Strait it is 4.5°C) On the other hand, boundary condition of the Aegean side of the domain, a problem seems to exist due to mesoscale eddies created and trapped because of the closed boundary conditions. However, we believe that this will not affect the Marmara basin because of short integration time length.

Our aim to understand the performance of non-hydrostatic terms in mixing of exchange flows in TSS. In our control simulation, we find that there are four different layers in the temperature field in the Dardanelle Strait whereas in the Bosphorus Strait, there are 3 layers seen as a result of density differences of two water distinct sources (Black Sea and Eagean Sea). In the salinity field of the Bosphorus Strait, vertical mixing effect is observed close to the surface waters in which salinity concentration is decreased. The interfacial layer between surface and deep layers is also increasing in thickness towards the Bosphorus Strait.

Circulation in the Marmara Sea is effected dominantly from jet flux issued to the Sea of Marmara from Bosphorus. Jet has three branches which splits into firstly to the west side of the Bosphorus Strait, opening of the Izmit Bay, secondly to southern boundary of the Marmara Sea by bending and converging with the big gyre in the middle and lastly to the North. This Northern branch also splits into two; one which directly flows

through the northern side of the Marmara Island and combined with small scale eddy by increasing its circulation speed and the other branch is shooting into the Marmara islands. This extended part of the jet also splits into many branches and flows into the entrance to the Dardanelle Strait. In our non-hydrostatic simulation, we find that the differences between two simulations are minor in the deep at this resolution. Surprisingly, the largest differences are close to the surface in terms of circulation and mesoscale eddy processes. The main reason behind this difference is resolving the evolution of vorticity using the full 3D vertical acceleration term in the non-hydrostatic simulation.



HİDROSTATİK VE HİDROSTATİK OLMAYAN TÜRK BOĞAZLAR SİSTEMİ SİMÜLASYONLARININ KARŞILAŞTIRILMASI

ÖZET

Türk Boğazlar Sistemi, Ege denizinin baseninden başlayarak Karadeniz'e ulaşırken Marmara denizini boğazlardan geçerek tamamlayan su yoluna verilen isimdir. Sistem denilmesinin sebebi ise, bu dinamik içerisinde bütün denizlerin, boğazların akışlarından oldukça etkilenmesinden dolayıdır. Karadeniz'in Marmara'ya ulaşmasında tek su köprüsü olarak görev yapan İstanbul Boğazı; rüzgar şiddetine, mevsimsel değişimlere, atmosfer basıncına ve Ege'den gelen suyun sıcaklık ve tuzluluğuna bağlı olarak akış debisi üzerindeki hacimsel farklılıklara sebep olan bu faktörlerden oldukça etkilenmektedir. Bunların sonucu olarak, Boğaz'ın Marmara'ya dökülen kısmında oluşan S şeklindeki yapıya jet adı verilir. Yön ve yoğunluğuna bağlı olarak Marmara'nın yüzeyindeki akıntı sistemini oluşturan bu jet, Ege'den ve Karadeniz'den gelen iki farklı özellikteki su kütlelerinin Boğazlar yoluyla Marmara'ya dökülmesiyle oluşan üçüncü bir su kütlelerinin karışımını doğrudan etkileyen bir yapı olması sebebiyle oldukça önem arz etmemektedir. Bu sistem boyunca su yoğunluklarına bağlı olarak düşeyde açıkça görülen bir tabakalaşma mevcuttur.

Bu çalışmada tabakalaşmalar Dardanel Boğazı içerisinde dört, Marmara denizi ve İstanbul Boğazı'nda üç adettir. Bu yoğunluk farklarının başlıca sebeplerinden biri Ege'den gelen tuzlu ve sıcak olan suyun yoğun olmasıdır. Bu yoğun su kütlelerinin Marmara'daki alt tabakadan ilerleyip İstanbul Boğazı'na ulaşmasıyla dikey kesitlerde görülen ve yüzeyde tuzluluk seviyesinin genel itibarıyla iyi karışmasından dolayı tuz derişiminin düştüğü gözlenmiştir. Buna ek olarak alt tabakada yoğun konsantrasyonunda bir tuzlu su sıkışmasının neden olduğu tuz oluşturmaktadır. Karadeniz'in soğuk ve az tuzlu suyunun Ege'den gelen su ile karışmasıyla oluşan ve boğazdan Marmara dökülen jet, üç ayrı kola ayrıldığı ve bu kolların Marmara denizindeki yapıların üzerinde etkisi olduğu yüzey kesitlerinden görülmüştür. Jet'in boğaz çıkışında, batıya İzmit Körfezi'ne yönelen ilk kolu küçük bir girdap oluşturmuştur. İkinci kolu ise Marmara Denizi'nin Güneyine doğru yol aldıktan sonra, ortasında büyük girdap ile birleşerek oradaki sirkülasyonun hızına katkıda bulunduğu gözlemlenmiştir. Üçüncü kolu ise ikiye ayrılmıştır; Güneyden kıvrılıp Marmara'nın kuzeyine giden bu kol önce Marmara adalarının arasında geçerek ada etkisi adı altında birçok alt kola ayrılarak Çanakkale Boğazına yönelmişlerdir, diğeri ise Kuzeye yönelerek Marmara adası ile Marmara Denizi'nin kuzeyindeki dar ve sığ şelf kısmında küçük ve güçlü bir girdap meydana getirmiştir. Bu çalışmada bu anlatılan etkilerin yüzeydeki ve derindeki etkisini gösteren bir okyanus modeline sahip olan MITgcm, TSS'nün bilinen üç boyutlu hidrostatik yaklaşımla yapılan modellerine ek olarak hidrostatik olmayan modellerinin de kullanılmasını sağlaması yönüyle diğerlerinden ayrılmaktadır. Bunlardan üç boyuttaki hidrostatik model olanı, Sannino et al. (2017) tarafından kullanılmıştır ve genel anlamda bizim hidrostatik olan modelimizin temelini oluşturmakla birlikte, arada farklılıklar da mevcuttur. Bunlardan ilki onların Karadeniz, Marmara ve Ege arasında olan düşeydeki farklılıkları gerçekte uyumlu

yapmak adına akış hacminde Karadeniz’de artış, Ege’de azaltma etkisiyle oluşturmuşlarken bizde bütün denizler aynı yükseltide bulunmaktadır. Bir diğeri ise, çeşitli akış hızları etkisi altında Marmara’daki sirkülasyonun ve oluşan yapıların değişimlerine ve olası nedenlerine bakmışlardır. Bu çalışmada ise, Sannino et al. (2017) aynı parametreler ile hem hidrostatik hem de hidrostatik olmayan iki model için 33 günlük simülasyona tabi tutulmuştur.

Navier Stokes denklemlerine çeşitli yaklaşımlar yapılmış olan hidrostatik modelden farklı olarak, hidrostatik olmayan modelde, düşeydeki hızın etkisi de göz önüne alınmaktadır ve daha küçük ölçekli yapıların gözlemlenmesi ile karışımın etkisinin artmasıyla yapılar hakkında daha ayrıntılı bir gözlem sağlanması amaçlanmıştır. Aradaki bu farkın ortaya çıkarılması açısından bu çalışma önem arz etmektedir. Hidrostatik olmayan modelden hidrostatik yaklaşımla elde edilmiş modeli çıkartarak bulduğumuz sonuçlara bakıldığında, hem yüzeydeki değişimleri ortaya çıkaran yüzey figürleri hem de düşeyde derinlikle olan değişimini görebildiğimiz dikey kesitlerde, yüzeye yakın kısımlarda az da olsa değişimlerin olduğunu gözlemlenmiştir. Buna ek olarak, Karadeniz'den gelen ve boğazdan akarak Ege’ye ulaşan bu soğuk ara tabakasının çevresinde düşeydeki karışımın artmasıyla değişimlere de olduğu da bulgular arasındadır. Bu çalışmadaki hidrostatik olan kısmın sonuçları Sannino et al. (2017) ile paralellik göstermektedir ve hidrostatik olmayan model arasındaki farklılıkları ortaya çıkarmak için yapılmış basit bir çalışmadır, Türk Boğazlar Sisteminin karmaşık dinamiğini ortaya koymaya çalışmamaktadır.

Sannino et al. (2017) oluşturdukları modelde Denizlere ait başlangıç koşullarını, Yaz döneminde yapmış oldukları CTD ölçümlerini baz alarak oluşturmuşlardır. Bu modele göre Karadeniz suyunun başlangıç koşulunda yeterince soğuk olarak verilmemesinden dolayı Denizlerdeki yüzey suları olması gereken sıcaklıklara ulaşamamakla birlikte kısa süreli simülasyonlarda gerçekçi sonuçlara ulaşamadığı görülmüştür. TSS’ye ait çalışmalar öncelikle Boğazların katkısının hidrolik olarak nasıl bir kontrol mekanizmasına sahip olduğunun anlaşılması için Boğaziçi’nde başlamıştır. Sistem olarak ele alınan modellerin yapılması önce Boğaziçi’nin 2 boyut için hem hidrostatik hem de hidrostatik olmayan modellerle elde edilen çalışmalardan sonra 3 boyuttaki hidrostatik modellerle Boğaz’ın dinamiğinin daha iyi anlaşılması amaçlanmıştır. Sonrasında hidrostatik olmayan modellerin de kullanılması TSS’nin sistem olarak ele alınmasının önemini dikeydeki ivmelenmeyi de katmasıyla ortaya çıkarmıştır. Bu yüzden bundan sonraki çalışmalar için daha ayrıntılı modeller hazırlanarak hidrostatik olmayan modeller üzerindeki farkın belirgin şekilde ortaya çıkması muhtemel görülmektedir. Bu dinamik içerisinde özellikle Marmara’nın tampon bölge olarak işlevini sürdürmesinin yanında ekonomik ve biyolojik çeşitlilik açısından da çok büyük önem arz ettiğini bilinmektedir. Karadeniz’in yağmur alması, çeşitli nehirlerin debisini akıtması ve zaman zaman ısı etkisi ile buharlaşmasının dengesini bulabilmesi için kanal yolu ile Marmara’ya boşalması bu dinamiği oluşturan parçaların Marmara’ya doğrudan bir katkısı olduğu yapılan çalışmalar doğrultusunda bilinmektedir. Marmara’nın, Türkiye’nin %25 ini de beslediğini göz önüne alırsak önemli bir ekonomik etken olması bu bölgenin dinamiğinin ayrıntılı incelenmesinin ve daha fazla fikir sahibi olabilmek için çeşitli modeller ile davranışını sistem içinde anlaşılması anlatılan nedenlerden ötürü hem Türkiye için hem de çevre denizlerini dolaylı yoldan etkileyebilmesi sebebiyle kıyısı olan diğer ülkeleri de etkilemektedir.

1. INTRODUCTION

There are two straits in Turkish Strait Systems (TSS) which are extending from east to west, namely Dardanelle Strait (DS) and Bosphorus Strait (BS), and a basin called Marmara Sea which interconnects these water pathways. Figure 1.1 shows the bathymetry map of the Marmara Sea. Having a large surface area, 11,500 km², variable bottom topography, maximum water depth is about 1350 m whereas minimum is 600 m, makes Marmara Basin a distinctive collector and distributor water body throughout Aegean Sea to Black Sea. There are three deep basins in the Marmara Sea. On the other hand, connecting straits are relatively shallow in depth and narrower in the width. Length of the Dardanelle reaches about 75 km while for Bosphorus is approximately only half of it. Thalweg lines which are the deepest part of the straits are shown in cyan and green lines for DS and BS, respectively. The red line in the Marmara Sea (Fig. 1.1) following through its depression the northern side is also used for cross section in model analyses.

Previous numerical studies have been done using hydrostatic and non-hydrostatic 2D numerical models. Recently, with the help of increasing performance of computing systems, 3D simulations are the main focus of the current models. In these advanced models, high resolutions are achieved with lesser computational costs even for finer scales. Recent models taking into account not only the additional effect of the vertical mixing but also the sharp stratification and change of thickness of these layers with changing characteristic within depth. MITgcm's hydrostatic solution is used by Sannino et al, 2017 in which initial sea level differentiation as well as relaxation values for salinity and temperature is arranged among three water masses according to their actual state by using CTD measurements taken during summer time, which is explained in their study in much more detailedly. In their case, various models are used for three-layer approximation under varying net flux but without wind forcing to understand the coupled behavior of the TSS in steady-state conditions.

In this thesis, we started from no flux case of the Sannino et al.(2017) study. In addition, we conducted a concurrent non-hydrostatic simulation to see differences in

terms of mixing, interfacial layer thickness, and depth, circulation changes. Finally, we take difference of the non-hydrostatic numerical model from the hydrostatic one to interpret the results accordingly. Although simulations are relatively idealized, we would like to isolate the impact of non-hydrostatic solution with removing wind forcing and surface volume fluxes. In the future, they can be extended to additional more complex cases.

In Chapter 2 previous studies related to modeling the TSS domain are reviewed. Briefly basic governing equations and descriptions are summarized for both our hydrostatic and non-hydrostatic models in the Chapter 3. For Chapter 4, usage of parameters and configuration of the model is explained detailed. Chapter 5 represents our result analyses not only for hydrostatic modelled domain but also for non-hydrostatic by making a comparison between the two. Chapter 6 explains general conclusions that are drawn from our findings after the showing differences also. Lastly in Chapter 7 gives suggestions about some other necessities other than our idealized non-hydrostatic model.

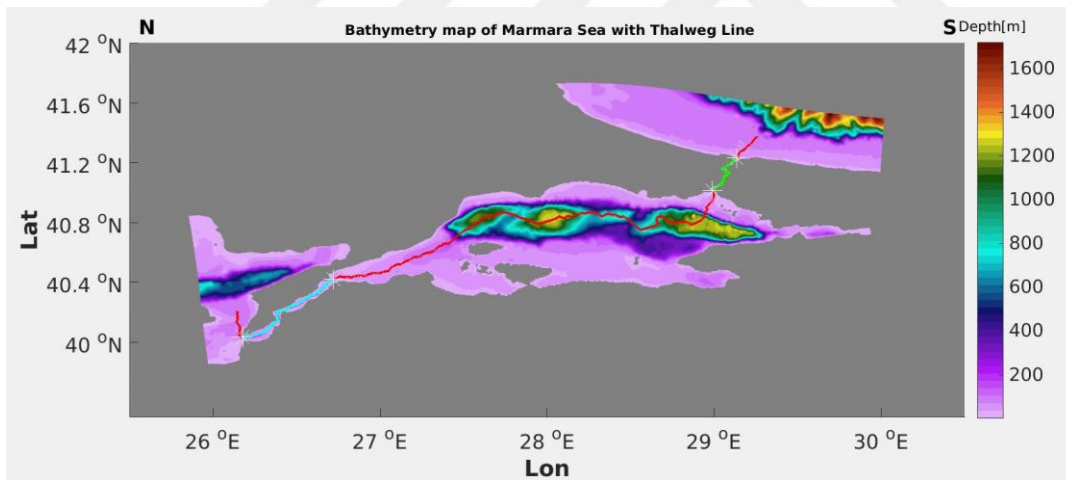


Figure 1.1 : Bathymetry map of the Marmara. Solid lines show: red for along the whole Thalweg line, cyan colored line (26.1806E 40.0328N -26.7199E 40.4193N) for DS and green one (28.9999E 41.0232N-29.1394E 41.2345N) for BS.

2. LITERATURE REVIEW

Hydrodynamics of the TSS is started to analyzed mathematically by Çeçen et al. (1981) and Bayazıt and Sümer (1982) but struggle to understand the flow from the Mediterranean Sea to Black Sea due to bad sampled data and lack of knowledge in complex topographic structures like canyons and sills. Importance of considering TSS as a dynamic system is understood only after by examining behavior of the flows distinctively either inflow or outflow of the straits to the both Black Sea and Aegean Sea which is supported from the studies of Demyshev and Dovgaya (2007), Demyshev et al. (2012) and Chiggiato et al. (2011). Although TSS has a small part comparison with global oceans, its density difference creates fast changes within the flow to the adjacent seas. Thus, separate impacts of the seas are investigated in a relation with the TSS by Beşiktepe et al. (1993, 1994, 2000) and Schroeder et al. (2012), on the other hand consequential effects of the coupled system to the Black Sea and Aegean Sea are reviewed by Ünlüata et al. 1990; Latif et al. 1991; Özsoy et al. (1995, 1996, 1997, 2001); Gregg and Özsoy (1999, 2002); Jarosz et al. (2011 a-b, 2012, 2013; Book et al. 2014 and Dorrell et al. 2016). Active tracers (temperature and salinity) exchange in terms of sharp interface between the mixed layers are observed in an 18 year simulated model to observe annually changed effects as well as S-shaped jet currents flow without taking into consideration of atmospheric forcing (Demyshev et al, 2012). In recent years, advancement in the computations lead detailed simulations resolving both small scale mixing and large scale circulation models and use extensively for TSS studies (Sannino et al, 2017; Gürses et al, 2016; Stanev et al, 2017, Aydogdu et al, 2018). Finite element model is tested under the influence of the both volume fluxes and atmospheric forcing and for its effect on the pycnocline depth variation in the Marmara Sea as integrated part of the TSS by Gürses et al. (2016). On the grounds of variability in topography of the Straits, high resolution curvilinear finite volume model is developed by Sannino et al. (2017) to investigate inflows of the energetic flows onto the Marmara Sea that causes turbulent mixing while considering hydraulic controls and jumps along narrow straits. Data assimilation is used to understand the nature of

the TSS especially of the Marmara Sea with atmospheric forcing with a 6 year of simulation in addition to forced fluxes of heat, water and momentum.

Depending on the discretized solution to the numerical models, problems are solved gradually in time with better understanding the structures and interpreting results more correctly. Water exchange flow dynamics which solve hydrodynamics equations for two layers in one-dimensional and two-dimensional numerical models are developed for Dardanelles (Oğuz and Sur, 1989; Staschuk and Hutter, 2001). Three-dimensional model flow simulations are developed for the Dardanelle (Kanarska and Maderich, 2008) and also for Bosphorus (Sözer and Özsoy, 2002; Oğuz, 2005; Sözer, 2013; Sözer and Özsoy, 2017). Ilıcak et al. (2009) developed a 2-D model which is averaged vertically for 3-D flows with smoother topography in Bosphorus. Investigating the similarities of the interchange of the flows in 2D have been studied for non-hydrostatic cases by Ilıcak and Armi (2010). In addition to hydrostatic models, non-hydrostatic models are in a need to resolve flow dynamics more realistically. Marshall et al. (1997a, 1997b) introduced different algorithms for hydrostatic, quasi-static and also non-hydrostatic model by using Navier-Stokes equations. Recently, to study the three-dimensional mixing in dispersive internal solitary waves and wave breaking near boundaries (Horn et al, 2001; Moum et al, 2003); cascade of 3D energy spectra from low wave numbers to high wave numbers (Muller et al, 2005); steep waves over rough topography (Beji and Battjes, 1994); buoyant plumes (Nash and Moum, 2005), deep convection (Marshall and Schott, 1999); 3D non-hydrostatic models were developed.

3. GOVERNING EQUATIONS

3.1 Introduction

In oceanography, it is important to understand the complex nature of the oceans with its coupled effects on the atmosphere. Thus, three-dimensional numeric hydrodynamic algorithms are introduced to overcome some of the difficulties firstly by making some assumption and approximation separately both in oceanic and atmospheric conditions. In this study, numerical simulations are performed to resolve flow dynamics in the TSS using primitive equations for hydrostatic and non-hydrostatic Reynolds averaged Navier-Stokes (RANS) equations. In this chapter, governing equations of the transport equation for tracers, conservation of mass, momentum and energy are summarized briefly.

3.2 Mathematical Formulations

Geophysical Fluid Movement theory is based on fluid mechanics and Newtonian mechanics which simplifies results according to conservation laws and acceleration of particle. Approximation leads less computational effort in numerical calculations. Thus, usage of Boussinesq approximation in Cartesian coordinate system eliminates the metric terms that comes from the spherical coordinates, ignores density difference and enables mass to be conserved in an incompressible way. Next section, we will introduce the governing equations which is solved numerically by the MIT General Circulation Model (MITgcm). After determination of the model domain, surface and lateral boundary conditions are applied to close the system. We also briefly discuss initial and boundary conditions at the end of this chapter.

3.2.1 Basic equations

The first equation is the conservation of mass which is the balance of rate of change of mass and net inflow of mass. This can be simply expressed as following;

$$\frac{1}{\rho} \frac{D\rho}{Dt} + \nabla \cdot \mathbf{u} = 0, \quad (3.1)$$

where D/Dt is the material derivative, ρ is the density and \mathbf{u} (u, v, w) is velocity vector in x, y, z directions which are eastward, northward and vertically upward, respectively.

According to Newton's second law, applied force on a fluid particle accelerates the particle and change its momentum in the fixed point in time;

$$\frac{D\mathbf{u}}{Dt} = \frac{1}{\rho} \mathbf{F} \quad (3.2)$$

Forces on a fluid could be categorized as i) body forces acting on per mass ii) surface forces that is caused by stresses applied on the fluid particle, or in response to cooling to a solid surface or another fluid particle;

Pressure force: $F_p = -\Delta p$ (Forces acting on sides of cubic volume)

Frictional force: $F_f = \nu \Delta^2 \mathbf{u}$ (Normal and shear stresses due to forces, inertial motion) where ν is the kinematic viscosity.

Body forces: $F_b = -g$ (Centrifugal force is incorporated in the true force of gravity) where g is gravitational acceleration

Coriolis forces: $F_c = 2\Omega \times \mathbf{u}$ (In the moving reference frame, particle motion is deflected) Ω is the rotation of Earth.

Adding these summarized forces into the right-hand side of the equation, we will get the momentum equations of motion;

$$\frac{D\mathbf{u}}{Dt} + 2\Omega \times \mathbf{u} = -\frac{1}{\rho_0} \nabla p + \mathbf{F}_b + \nabla \cdot (\boldsymbol{\nu} \nabla \mathbf{u}) \quad (3.3)$$

In the ocean, the density is computed using a non-linear equation of state (Jackett and McDougall, 1995) which is a function of temperature, salinity and pressure;

$$\rho = \rho(T, S, p). \quad (3.4)$$

Temperature (T) equation is governed by the advective-diffusive equation

$$\rho C_v \frac{DT}{Dt} = k_T \nabla^2 T \quad (3.5)$$

ρ where C_v is the heat capacity and k_T is the thermal conductivity of the fluid. Similar to the previous equation salinity (S) equation as follows

$$\frac{DS}{Dt} = k_s \nabla^2 S \quad (3.6)$$

Above equations describes how to solve the equation with 7 unknowns: In the three momentum equations are for (u, v, w), energy equation is for T, salt conservation for (S), continuity equation for (p).

Writing in the Cartesian coordinates of the momentum equations this time including water moving under the Coriolis effect;

$$\frac{Du}{Dt} + wf_H - vf_V = \frac{1}{\rho} \frac{\partial p}{\partial x} \quad (3.7)$$

$$\frac{Dv}{Dt} + uf_V = \frac{1}{\rho} \frac{\partial p}{\partial y} \quad (3.8)$$

$$\frac{Dw}{Dt} + uf_H = \frac{1}{\rho} \frac{\partial p}{\partial z} - g \quad (3.9)$$

where Jankowski (1999) shows the Coriolis force,

$$F_c = \begin{pmatrix} 2w\Omega \cos \varphi - 2v\Omega \sin \varphi \\ 2u\Omega \sin \varphi \\ 2u\Omega \cos \varphi \end{pmatrix} = \begin{pmatrix} f_H w - f_V u \\ f_V u \\ f_H \end{pmatrix} \quad (3.10)$$

Note that, generally f_H terms are neglected since they are relatively small compared to f_V in the rotation terms in the equations of motion.

3.2.2 Boussinesq approximation

Within the ocean, density of sea water changes approximately 5%. Thus, we can assume that in the inertial terms, and in the continuity equation, we may substitute

ρ_0 , a constant. However, even small changes in density is important in buoyancy, and so we retain variations in density in the buoyancy term of the vertical equation of motion. This is called Boussinesq approximation which can be assumed as compressibility is rather small in the oceanic flows and can be neglected. Mathematical descriptions are follows;

$$\frac{\partial v}{\partial t} + \mathbf{u} \cdot \nabla u - v f_V + w f_H = -\frac{1}{\rho_0} \frac{\partial p}{\partial x} + \nabla \cdot (\mathbf{v} \nabla u) \quad (3.11)$$

$$\frac{\partial v}{\partial t} + \mathbf{u} \cdot \nabla v + u f_V = -\frac{1}{\rho_0} \frac{\partial p}{\partial y} + \nabla \cdot (\mathbf{v} \nabla v) \quad (3.12)$$

$$\frac{\partial w}{\partial t} + \mathbf{u} \cdot \nabla w - u f_H = -\frac{1}{\rho_0} \frac{\partial p}{\partial z} - g + \nabla \cdot (\mathbf{v} \nabla w) \quad (3.13)$$

Using the conservation of mass principle, continuity of fluid motion in time for an incompressible fluid flow with constant fluid density is written in the form;

$$\frac{D\rho}{Dt} = 0 \quad (3.14)$$

Thus, continuity equation for an incompressible fluid (3.1) reduces to incompressible form;

$$\frac{\partial w}{\partial t} + \mathbf{u} \cdot \nabla w - u f_H = -\frac{1}{\rho_0} \frac{\partial p}{\partial z} - g + \nabla \cdot (\mathbf{v} \nabla w) \quad (3.15)$$

$$\nabla \cdot \mathbf{u} = 0 \quad (3.16)$$

Above equations 3.11-3.13 and 3.3 are called non-hydrostatic equations with Boussinesq approximation.

3.2.3 Hydrostatic approximation

Due to the ratio of horizontal length (L) to vertical depth in the ocean (H), vertical acceleration terms and viscosity and turbulent stresses can be neglected using the scale analysis. Pressure is balanced with the water column depth. Thus, the equation 3.12 becomes;

$$\frac{\partial p}{\partial z} = -\rho g, \quad (3.17)$$

where the force of gravity is balanced by vertical component of the pressure gradient force.

3.2.4 Boundary conditions

The model is initialized from rest ($u=v=w=0$), with three different water masses (T,S, ρ) in the Aegean Sea, Marmara Sea and Black Sea regions. We employ no-slip closed boundary conditions for the lateral boundary conditions i.e. tangential components of velocity around solid boundaries are zero.

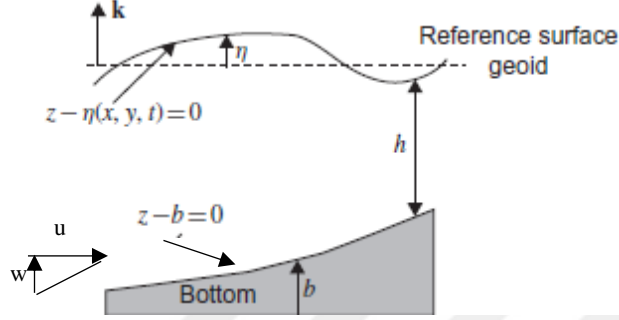


Figure 3.1 : Illustration of bottom and surface boundary notation. Moving surface is impermeable while $z=\eta$ in 3.15, taken from Cushman Roisin et al. (2011)

In addition to no-slip conditions, no flux conditions are also used when dealing with initial and boundary conditions in the closed domain. Simplistic formulas are follows for the upper and lower conditions:

Surface boundary condition:
$$w = \frac{\partial \eta}{\partial t} + u \frac{\partial \eta}{\partial x} + v \frac{\partial \eta}{\partial y} \quad (3.18)$$

Boundary condition at the bottom:
$$\frac{\partial}{\partial t}(z - b) = 0 \quad \left(\frac{dz}{dt} = w \right) \quad (3.19)$$

At the free surface:
$$\frac{\partial}{\partial t}(z - \eta) = 0 \quad (3.20)$$

Surface boundary conditions for momentum and buoyancy (T and S) are also set to zero, thus no wind effect, heating/cooling and evaporation/precipitation.



4. MODEL CONFIGURATION OF THE NUMERICAL MODEL

We use both hydrostatic and non-hydrostatic versions of Massachusetts Institute of Technology general circulation model (MITgcm) is with the Boussinesq approximation. The MITgcm is a three-dimensional Arakawa C-grid fully incompressible Navier-Stokes equations model (Marshall et al, 1997). Finite volume discretization has been used in the horizontal, while in the vertical the MITgcm has a z-star vertical grid (Adcroft and Campin, 2004) which is a fully nonlinear free surface implementation which allows one to deal with large amplitude free-surface variations relative to the vertical resolution.

Model domain covers the area from Dardanelle Strait to Bosphorus Strait connection with the Marmara Sea. This model is taken over from the Sannino et al. (2017) study but in addition to their research, it is also aimed to understand the behavior of the model in non-hydrostatic setup. Initial conditions are based on the sampled data , CTD, from the three water masses Eagen Sea, Marmara Sea and Black Sea respectively in the summer. Thus, surface warm waters are not able to reached climatological values especially in the Black Sea because of that initialization of layers changing with depth. On the other hand for the surface water temperature values, apart from the summer time, rest of the months seems to be colder in average that of summer. The case measurement for the model initialization is taken in special time of the year where water masses more calmer and warmer. Since both models are integrated only 33 days, surface waters are not sufficiently affected by cold water of the Black Sea. On the Eagen side, closed boundary conditions do not allow mesoscale eddies leave the domain, however short integration time ensure that results in the Marmara Sea will not contaminated. Bathymetry data is provided by Turkish Navy, Navigation, Hydrography and Oceanography Office in the Straits for Erkan Gökaşan (Gökaşan et al. 2005, 2007) has a resolution of 20 meter, while in the Marmara Sea resolution changes to 30 arc-seconds with having a grid of General Bathymetric Chart of the Oceans GEBCO. In this study, structured curvilinear mesh grid has been used. The model setup domain extends from 26° from the NE of the Aegean Sea to the 30° of

the NW Black Sea and 39°30' to 42° N in the meridional direction. Total grid points are 1728 in x-direction and 648 in y-direction with ranging resolution from close to 50 m in Straits, about 1 km in the Marmara region. Figure 4.1 shows every 5 points of the actual number of grid points that belongs to the model domain. This figure also shows, how distinctively distributed the grid is. Starting in the Northern side where the Black Sea is attached with the MS, grid is much confined, thus have a higher resolution along the Bosphorus Strait. Whereas in the northern side of the Marmara Sea, three elongated deep basins are the target of interest due to the slope of the bottom surface is changing fast comparison within the whole basin, grid is much less but wider. Although this resolution is enough for observing the vertical changes with mesoscale features in the Marmara Sea, the grid is relatively coarse in the Dardanelle Strait. Besides, Southern sides of the Marmara is also relatively coarse, for this reason resolution is not sufficient in here as well. In addition, the grid resolution is expanded at the end of the model domain where is the small part of the Aegean Sea included.

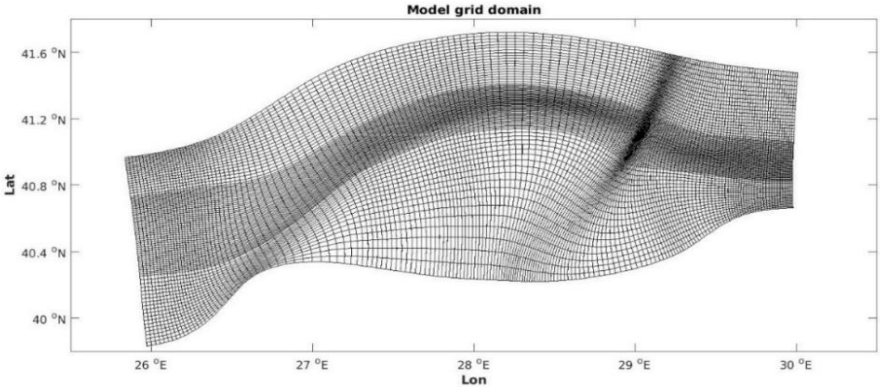


Figure 4.1 : Model grid domain of the study area.

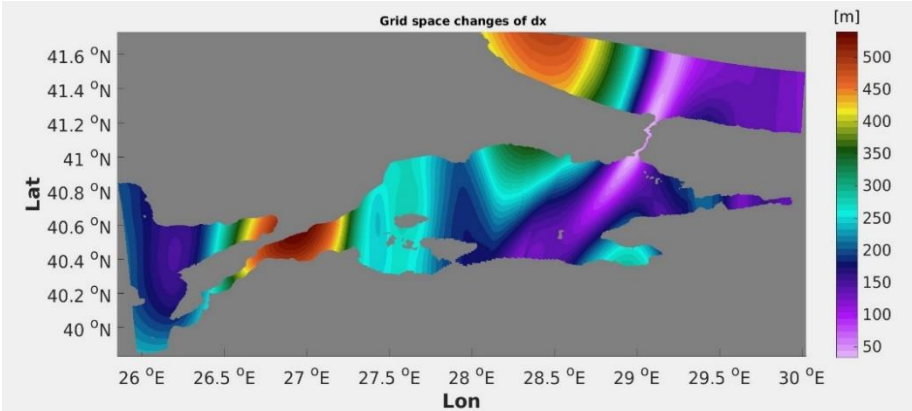


Figure 4.2 : Grid spacing in the x-direction (dx) of model domain

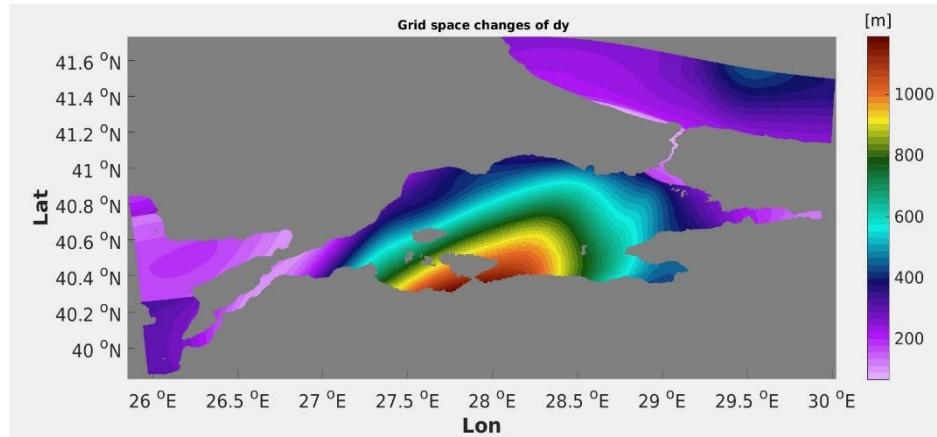


Figure 4.3 : Grid spacing in the y-direction (dy) of model domain.

Grid spacing in the x-direction and y-direction is given in the Figures 4.2 and 4.3 respectively. These figures show how the lateral resolution, in meters, changes in both directions. Black Sea has coarser resolution (~ 450 m in x, ~ 200 m in y) in the west and gradually increases in resolution (up to ~ 50 m in x, ~ 100 m in y) where it enters into the Bosphorus. Entrance of the Strait to the Marmara Sea, resolution decreases gradually except in the deeper basins in the north (~ 250 m in x, ~ 550 m in y) and shallower parts in the east (~ 150 m in x, ~ 150 m in y) in Gulf of the Izmit. Close to the DS, fine resolution is enhanced starting from the Marmara island (~ 250 m in x, changes from 550-100 m in y) and along the DS resolution in x-direction reaches up to 500 m while in the y-direction is around 100 m. This resolution is relatively low in comparison to the Bosphorus. West of the DS, resolution again decreases in x-direction as near as 150 m in northern side whereas in y, no changes is observed. In the vertical, the model has 100 unequal z-levels where thicknesses of the levels change exponentially from 1.2 m at the surface to 110 m at the bottom (Sannino et al, 2017). These levels of distribution in the water column provides that vertical resolution will be much higher in the shallower part of the sea (first 100 m) covering first 50 levels in taking consideration of the Straits. While the rest of 50 levels are discretized in a rather sufficiently resolution in the vertical direction in basin of the Marmara's variable topography. Increased vertical resolution at the upper part of the ocean helps us to distinguish mixing in the interfacial layer which is in between surface layer and deep layer since density differences between these interfaces obviously seen with this model configuration.

In the model's boundary conditions, tangential and normal velocity components at the solid boundary taken as zero (according to no-slip condition application) in the

momentum and tracer equations together with application of no flux (insulation) condition as the closed boundaries. A third order flux limited tracer advection scheme is selected for the tracer advection operator (Hundsdorfer et al, 1995), similar to the numerical experiments of non-hydrostatic simulations in Strait of Gibraltar (Sanchez-Garrido et al, 2011; Sannino et al, 2014). We choose turbulence closure from Dorrell et al, 2016) for vertical viscosity and diffusivity values based on shear-driven mixing. Horizontal viscosity variation is considered from Leith (1968). Implementation of the model algorithm was explained in the early chapter (chapter 3). In addition to hydrostatic model, non-hydrostatic model is also implemented with the same parameters used in Sannino et al. (2017). Thus, in this section only parameters that is chosen for hydrostatic model will be showed in the table. Similar to the Sannino et al. (2017) model setup, initialization of the model starts with three different water masses at the same level (no vertical variations) and also net volume flux at the surface is kept zero in the simulation, i.e. no sea surface height forcing between Black Sea and Aegean Sea. Our aim is to understand the basic difference between non-hydrostatic and hydrostatic models, hence the simplest case of scenario is used by not considering the effects of external forcing or tidal effects implementation. Simulations have been integrated for 33 days and exchange of water masses is allowed to became a steady state with time.

Table 4.1 : Model parameters used in TSS

	Value	Unit	Description
A_h	2×10^{-2}	$m^2 s^{-1}$	Horizontal viscosity coefficient
C_d	0.02	-	Bottom drag
A_v	1.5×10^{-4}	$m^2 s^{-1}$	Vertical background viscosity
K_v	1×10^{-5}	$m^2 s^{-1}$	Background diffusivity
Δt	5	s	Time step

5. INTERPRETATIONS AND RESULTS

In this chapter, numerical analyses obtained from the MITgcm model show the results of tracer distribution (in here only as salt and temperature) within sections in terms of depth and distance and surface plots as latitude and longitude in the model domain of TSS. Simulations are based on hydrostatic and nonhydrostatic models to investigate the hydrodynamics under the same parametrization that is discussed in chapter 4. The main objective of this study is to make a better comparison in 3D simulation of Reynolds Averaged Navier Stokes of TSS for understanding the benefits that will come from the control experiment considering an ideal model setup. We present below a number of such results taken across various sections determined from two ends of the Straits along with a few surface plots of the integrated model configuration. We analyzed 5 days averaged results after 33 days of integration time.

5.1 Numerical Model Results with Hydrostatic Solution

Vertical sections in the following figures show behavioral characteristics of salinity (S) and temperature (T) distribution differs throughout three water bodies (Dardanelle, Marmara, Bosphorus) over the whole domain with the specified initial conditions. After steady state condition is satisfied over a monthly simulated model, we can distinguish the differences of the interfacial layers better. These layers are observed along straits and also in the Marmara basin due to the tracer contents (T,S) of the two different water sources.

5.1.1 Temperature and salinity distribution along the Dardanelle Strait

Figure 5.1 shows the temperature and salinity fields as a vertical cross section at the Dardanelle Strait. There are four distinct water masses in the temperature field (Figure 5.1A). At the surface, there is the warm surface water (approximately 23 °C), and below that there are two intermediate water masses; one is a cold tongue (14 °C) coming from the Marmara Sea and the other one is intermediate warm water from Aegean Sea (20 °C). The relative cold deep water (17 °C) lies below all these three water masses. It is hard to see the same four-layer structure in the salinity field in the

Dardanelle Strait (Figure 5.1B). There are only three layers are visible: i) fresh surface layer coming from Black Sea (22 psu) ii) salty deep layer flowing from Aegean Sea (38 psu) iii) interfacial layer in between. Density isopycnals are raised slightly around 50km (approximately Nara Burnu), and south of that the interfacial layer is thickening which is an indication of diapycnic mixing. Interfacial layer depth and thickness changes depending on the inflow and outflow values and also to the bottom topographic slopes. Since there is no wind forcing in this experiment, there is no blocking events in both Straits. The flow is adjusted by density differences.

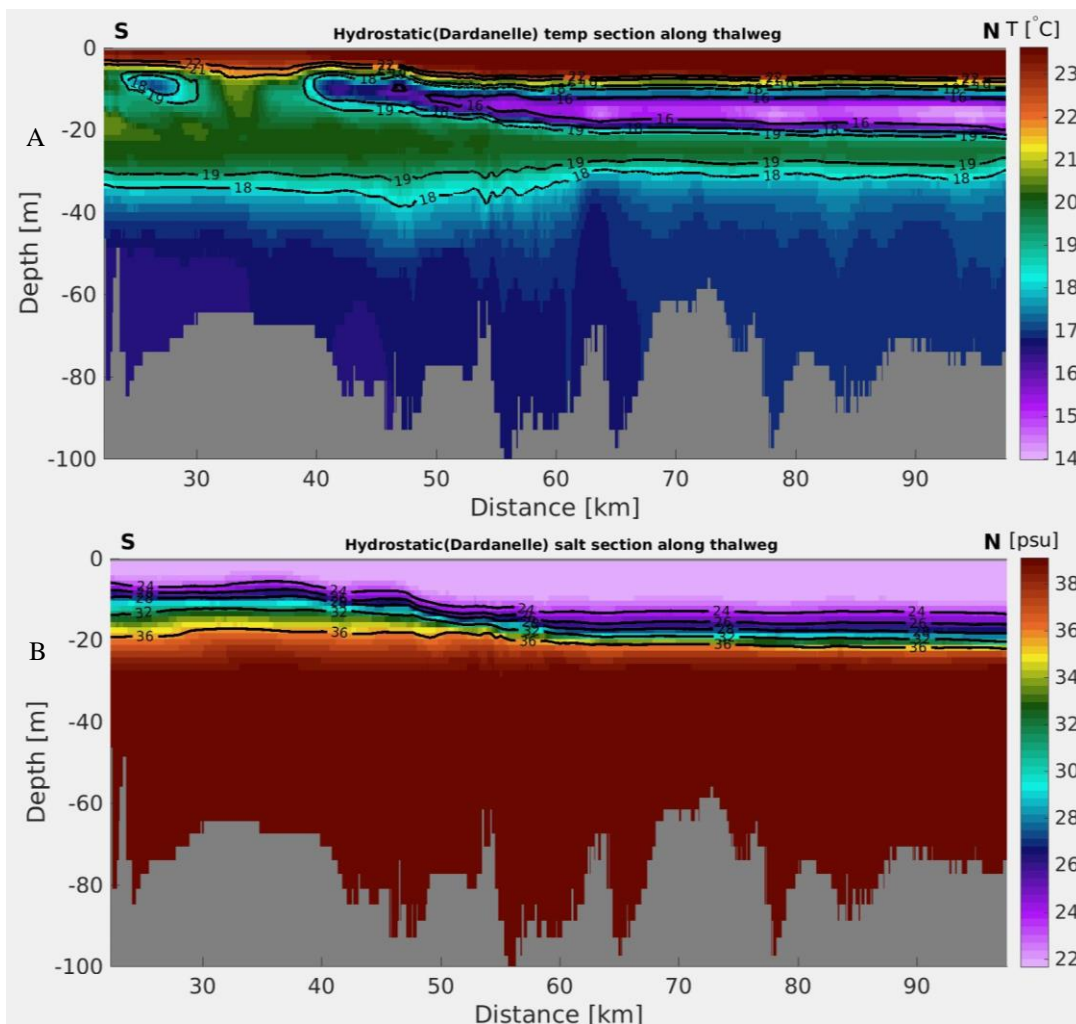


Figure 5.1 : Time averaged section (A) for Temperature and (B) for Salinity between two chosen coordinates in Figure 1.2 along thalweg line for Dardanelle with no barotropic volume flux. Black lines show contours and the numbers on them show their values.

5.1.2 Temperature and salinity distribution along the Bosphorus Strait

Figure 5.2. displays the temperature and salinity fields at the Bosphorus Strait. There are three different water masses in the Strait.

The warm/salty Mediterranean Sea water is at the bottom. There is the fresh and cold tongue (10 °C) at the intermediate layer and warm and fresh Black Sea water at the surface. There are two hydraulic control locations at the Bosphorus; one is a narrow contraction at $x=373$ km (where the channel is deepest) and the other is the sill at exit of the Strait into the Black Sea ($x=394$ km). A hydraulic jump is visible at the contraction location in the isohalines between two layers of the Black Sea water. The interfacial layer between bottom layer and surface is increasing flowing to the Black Sea exit, while salinity values are decreasing in the bottom layer. Cold intermediate layer coming from the Black Sea also warming up close to the Marmara exit of the Strait. Once again, this is a clear indication of vertical mixing between two different water masses. At the sill location, the steepening of the isopycnals are relatively limited. This might be due to location of the thalweg, however further investigation is required.

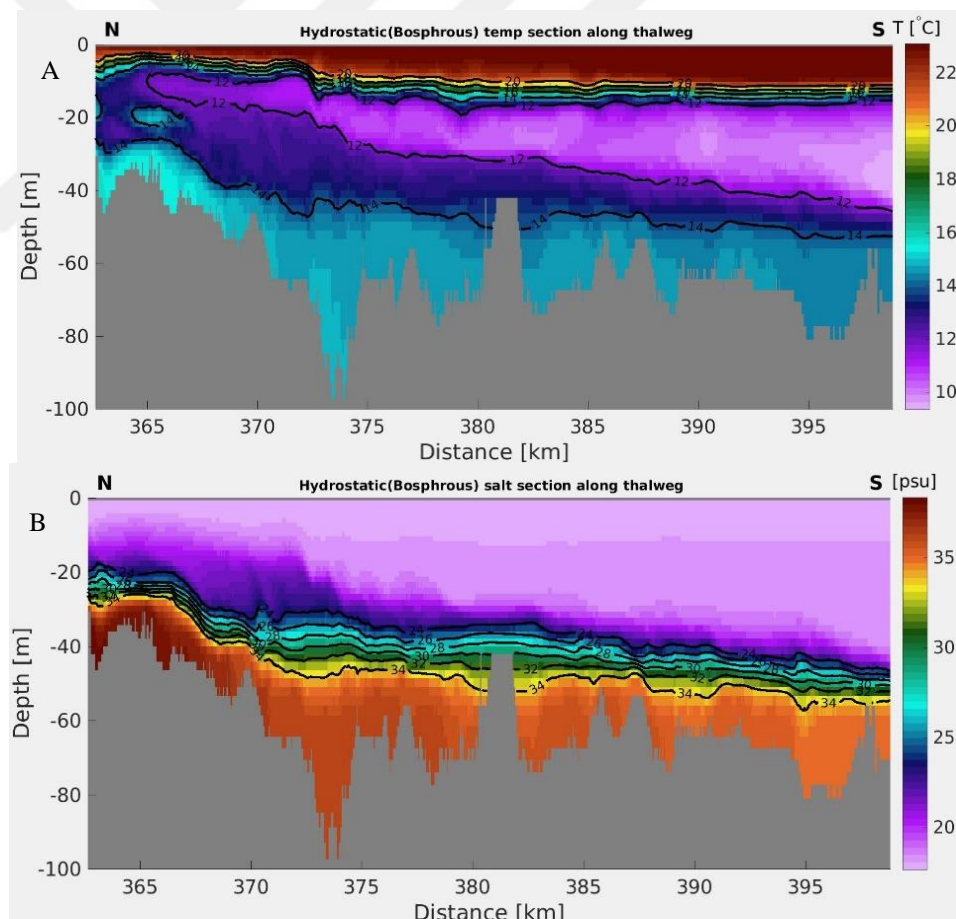


Figure 5.2 : Temperature section(A) and Salt section(B) between two chosen coordinates in Figure 1.2 along thalweg line for Bosphorus Strait with no barotropic volume flux.

5.1.3 Temperature and salinity distribution along the TSS

The vertical sections for salinity and temperature along the thalweg line (shown in Fig. 1.1) are shown in Fig. 5.3. We show the active tracer fields focusing on the upper 150-meter depth Figs. 5.3 C and D. The upper surface layer remains less than 25 meters along the section. The cold subsurface layer which was from previous winter is visible in the Marmara Sea. This layer mixes with the warm Dardanelle Strait subsurface water and gets diluted in the DS. Four-layer temperature structure can be seen west side of the Marmara Sea interior. Salinity mixes rapidly in the Bosphorus Strait compared to the Dardanelle and Marmara Sea regions. Note that colorbars are different than those in Figs. 5.1 and 5.2 to distinguish the different water masses.

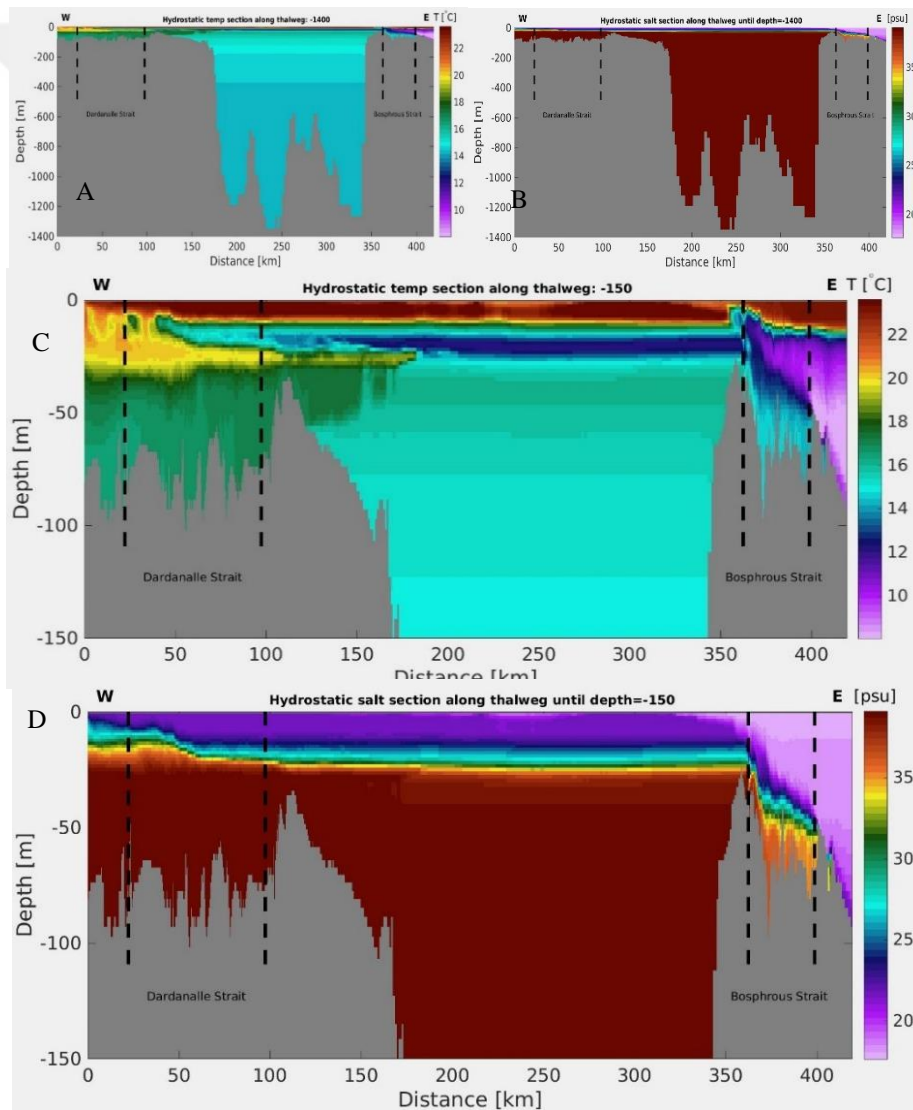


Figure 5.3 : Sections of Salinity (B,D) and Temperature (A,C) along Thalweg line which includes starting from Mediterranean sea, Dardanelle Strait, Marmara Sea and Bosphorus Strait to come an end in the Black sea respectively.

5.1.4 Sea surface height and vorticity of the Marmara Sea

Sea surface height field shows a basin scale gyre at the center of Marmara Sea, a small eddy north of Marmara island, a jet feature exit of Bosphorus and another eddy entrance of Izmit Bay (Figure 5.4). The Bosphorus Jet overshoots and impinges on the Bozburun peninsula on the south side of the Marmara Sea. After that, the flow joins into the central gyre in the basin. The results are similar to a buoyant outflow out of a geometric constraint and creates an anticyclonic gyre. This feature is similar to the Alboran Gyre in the Mediterranean Sea.

We decided to investigate circulation of the Marmara Sea in detail. To this end, surface relative vorticity,

$$\xi = \nabla \times u_h = -\frac{\partial u}{\partial y} + \frac{\partial v}{\partial x} \quad (5.1)$$

is computed and standardized by dividing Coriolis force (ξ/f) plotted in Figure 5.5. It is defined as, when $\zeta > 0$, the flow is cyclonic (counter-clockwise), and for $\zeta < 0$, it is anti-cyclonic (clockwise). In addition to the eddies and gyre mentioned above, we can see multiple eddies at the western boundary in the Aegean Sea and island effects around Imrali, Ekinlik, Avsa islands in the Marmara Sea. Eddies in the western boundary cannot leave the domain because of closed boundary conditions. Normalized vorticity (ξ/f) values indicate geostrophic motion (approximately 2D) if they are less than unity, however when normalized vorticity reaches to -1 and 1 at the exit of both Straits, we can conclude that motion is ageostrophic (3D in nature).

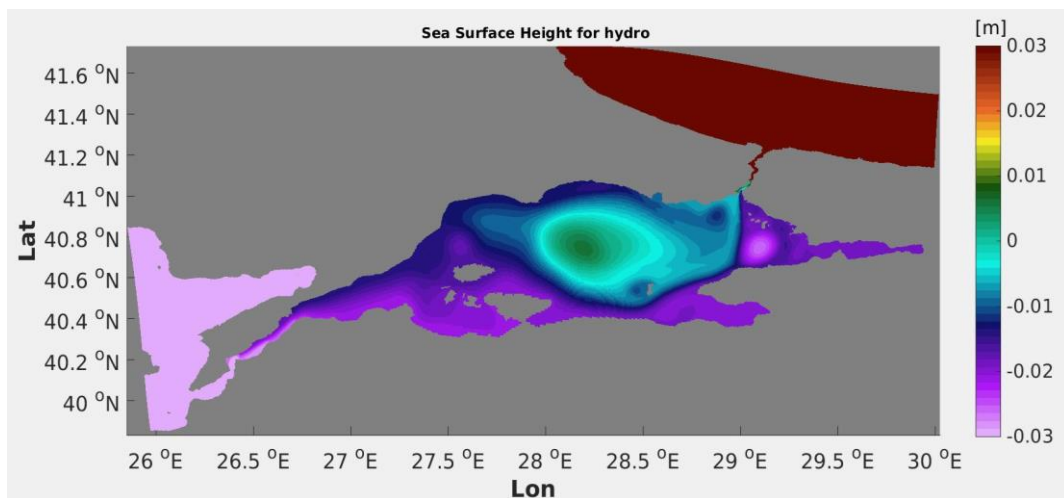


Figure 5.4 : The mean sea surface height field.

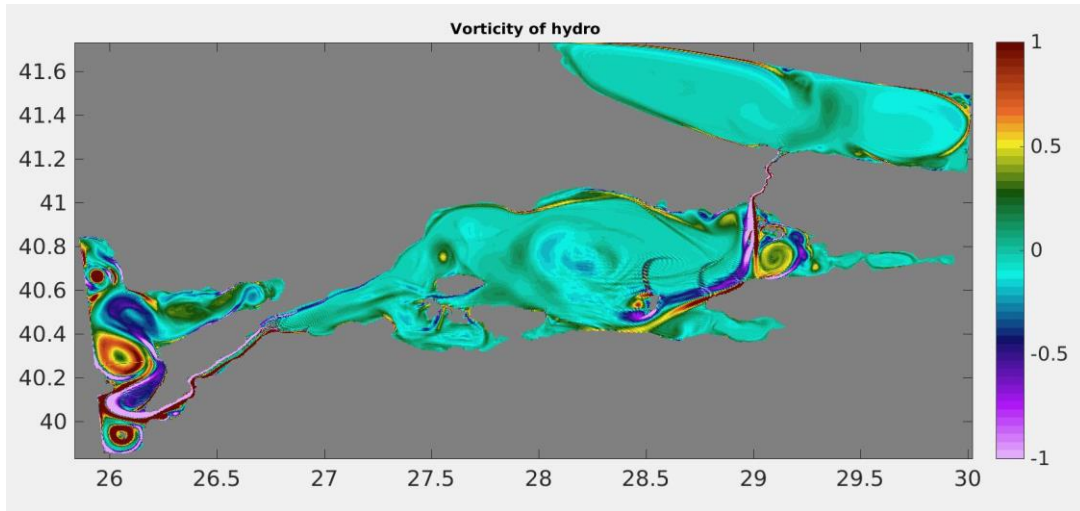


Figure 5.5 : The mean relative vorticity normalized by the Coriolis force.

5.2 Comparison of Hydrostatic Simulation with Non-Hydrostatic Simulation

The model analyzed in previous sections is different to the one proposed by Sannino et al. (2017), who studied the hydrostatic model dynamics of TSS. They are using various amounts of fluxes and taking into account of vertical heights of the Straits and Marmara Sea by adding water, to the Black sea, and subtracting water from the Dardanelle. In this section, we conduct a new non-hydrostatic simulation with addition of the nonlinear terms in the vertical momentum equation. This model investigates whether the importance of vertical velocity or its turbulent entrainment mechanism effected by the non-hydrostatic terms at this grid resolution.

5.2.1 Temperature and salinity distribution along the Dardanelle Strait

Below sections are obtained subtracting the non-hydrostatic model from hydrostatic one to investigate the differences between two model simulations. This numerical study highlights the behavior of the system where the temperature and salt values differs in Straits and the Marmara Sea. Results of the model show that averaged temperature as well as salt values changing from -0.04 to 0.04. On the other hand, in TSS sections, the values merely exceed to 0.25 °C in temperature and 0.25 psu in salt concentration. TSS sea surface temperature field shows change of values approximately 3 °C in the Marmara basin while salt concentration ranging from -1 to 1 psu in the same region (not shown). SSH difference is very low in about the order of 10^{-3} .

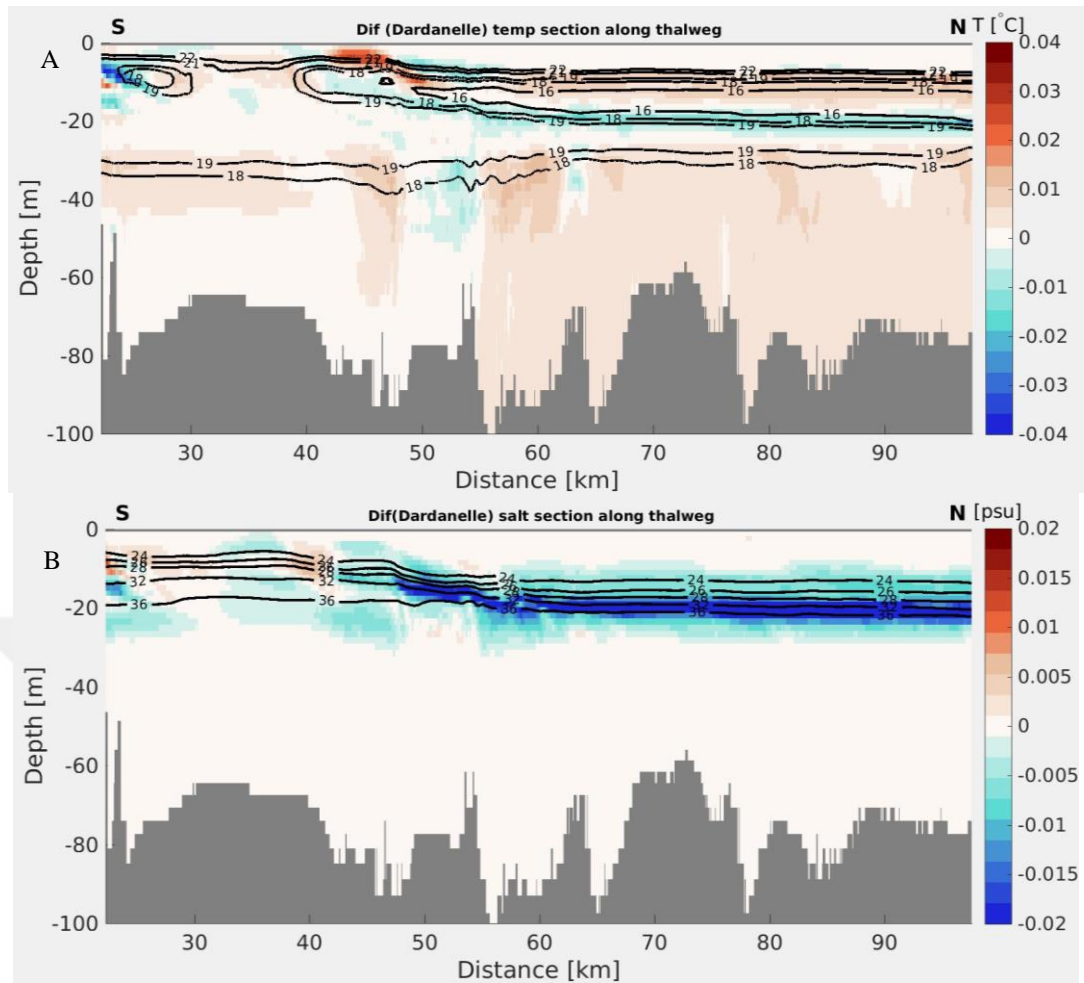


Figure 5.6 : Temperature section (A) and Salt section (B) difference of Dardanelle along thalweg with no flux.

Figure 5.6 shows the vertical cross section of temperature field between non-hydrostatic and hydrostatic simulations. Black contours are isohalines from the hydrostatic model. The deep water is slightly warmer/saltier in the sensitivity experiment. On the other hand, cold intermediate layer coming from the Marmara Sea is colder and fresher in the non-hydrostatic simulation. This is due to the mixing of the subsurface water in the central Marmara basin. By looking closely to near of the Nara pass region, increase/decrease in temperature/salinity can be seen as additional difference. Also, in the southern side of the section, entrance to the Aegean Sea, water seems to be colder and saltier in comparison to hydrostatic case.

5.2.2 Temperature and salinity distribution along the Bosphorus Strait

Figure 5.7 shows the difference of temperature and salinity fields in the Bosphorus Strait. Temperature field does not display significant difference except the interfacial layer between surface Black Sea water and intermediate cold water.

The latter upwells slightly and replaces surface water. There is a dipole shift in the salinity field between two simulations. Density difference between upper and lower layers are reduced as the lower layer gets fresher and upper layer gets saltier. This leads us to conclude that whole water column mixes vertically in the non-hydrostatic simulation.

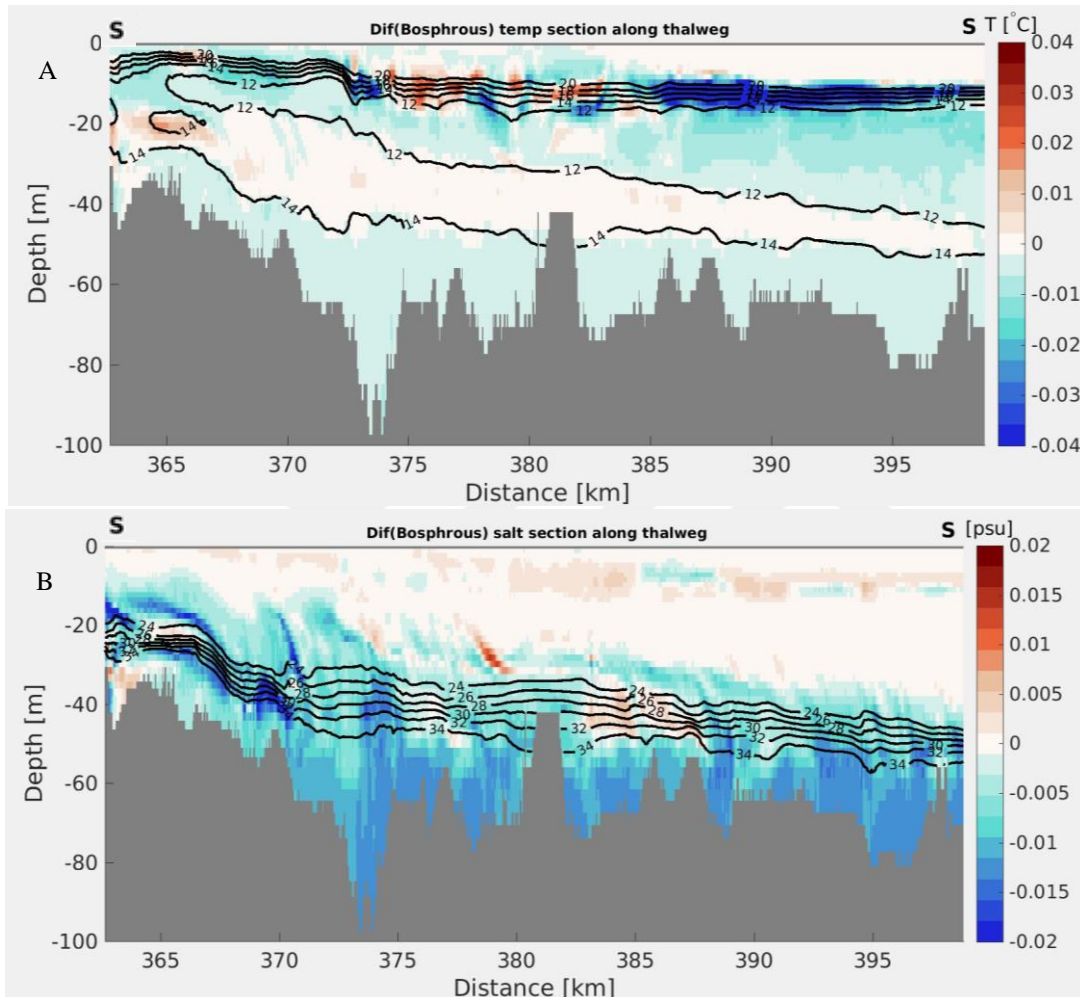


Figure 5.7 : Temperature section (A) and Salt section (B) difference of Bosphorus along thalweg with no flux.

5.2.3 Temperature and salinity distribution along the TSS

In this section, we analyze the salinity and temperature differences between two models along the thalweg section over the whole domain (Figure 5.8). The largest difference in temperature field between two simulations is at the center of the basin where the basin scale gyre sits in. Circulation strength of the gyre seems to be shifted towards to the southern side of the Marmara Sea. This locality change has also been directly related to the shifting of the Bosphorus jet.

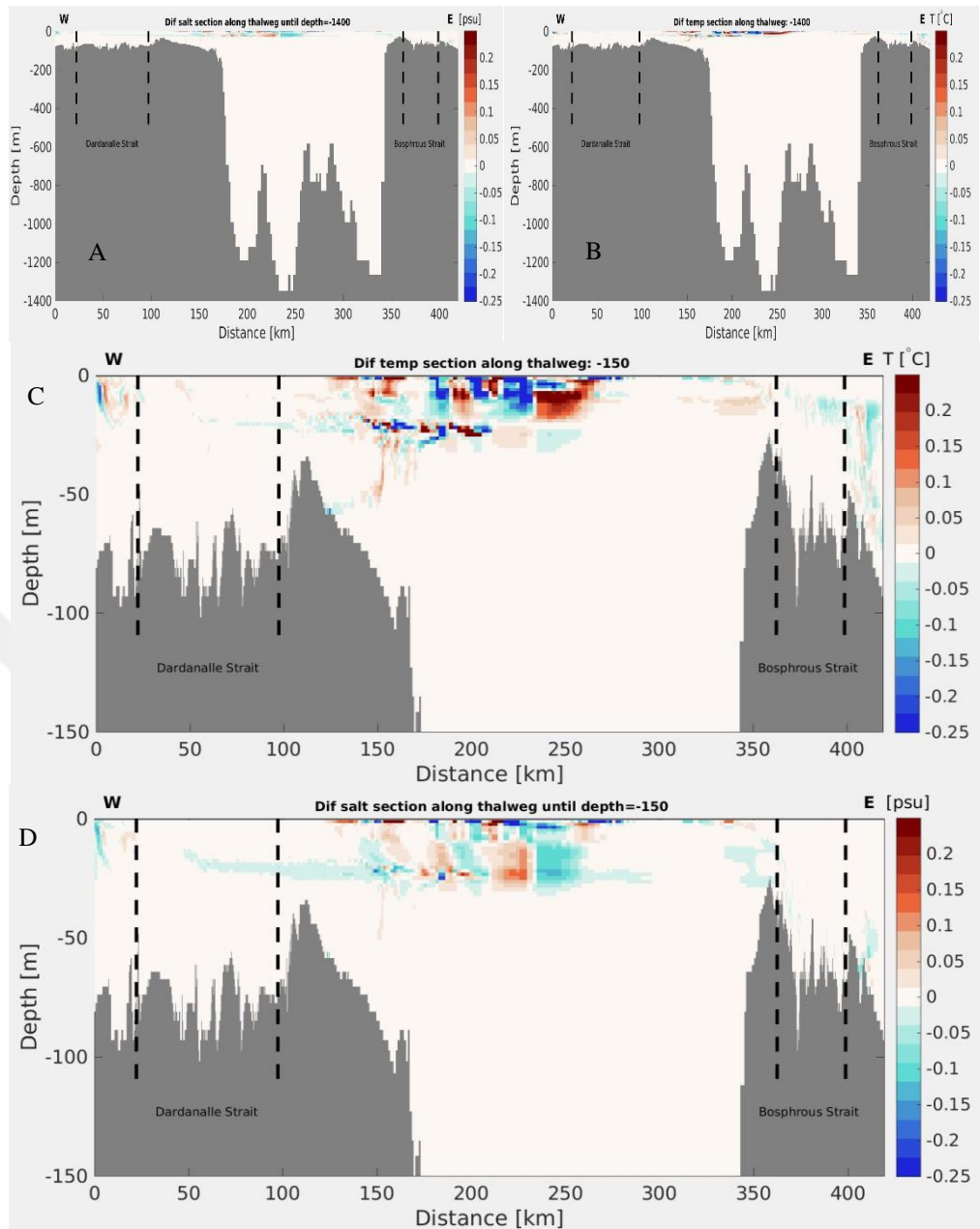


Figure 5.8 : Sections of difference for Salinity (B,D) and Temperature (A,C) along Thalweg line.

Area of the closed circular region of the gyre gets smaller, although we have to note that the difference is minor. The difference can be up to 0.8 degrees Celsius.

Change in upper surface layer indicates the gyre properties change on the surface. Accompanied salinity field difference also supports this finding. Figure 5.8D displays 0.25 psu changes in the upper 25 salinity and some freshening at the subsurface layer flowing into the Dardanelle Strait. To see the difference in the central basin gyre, we decided to study sea surface height and sea surface vorticity in the next section.

Time equation of the k-component of the vorticity field in three-dimensional case is:

$$\begin{aligned} \frac{d}{dt}(\xi + f) = & -(\xi + f) \left(\frac{\partial u}{\partial x} + \frac{\partial v}{\partial y} \right) - \left(\frac{\partial w}{\partial x} \frac{\partial v}{\partial z} - \frac{\partial w}{\partial y} \frac{\partial u}{\partial z} \right) \\ & + \frac{1}{\rho^2} \left(\frac{\partial p}{\partial y} \frac{\partial \rho}{\partial x} - \frac{\partial p}{\partial x} \frac{\partial \rho}{\partial y} \right) \end{aligned} \quad (5.2)$$

where the first term of the right-hand side is the effect of horizontal velocity divergence on vorticity, the second term is the transfer of vorticity between horizontal and vertical components (“tilting term”) and the last one is the effects of baroclinity (“solenoidal term”). In a fully non-hydrostatic model, vertical velocity in the second term should be significantly different than the diagnostic version of the vertical velocity. This leads to significant changes of circulation and tilting between upper and lower layer in the Marmara Sea. We believe this is the reason that major differences in temperature and salinity are confined in the gyre area and upper 25 meter.

5.2.4 Sea surface height and vorticity of the Marmara Sea

Sea surface height changes accordingly with the water column thickness. These observed changes in three different regions in the Marmara Sea as a consequence of alignment to the right of the Bosphorus jet. In Figure 5.9, northern side of the Marmara island, height difference is easily distinguishable between the two water masses; one is more circular and relatively lower whereas the other is related to balancing of these low level surface of difference by ascending. In addition to that, in the middle of the Marmara Sea, behavior of the gyre and SSH difference have an indication that gyre shifted to the right. This also is observed in the vorticity map (Figure 5.9). SSH decreased and observed as a circular structure at the entrance of the gulf of Izmit (where the self gets shallower and ends in chaotic behavior). These differences are consequence of the shift of the Bosphorus jet to the right. Since the jet is the main driving circulation force in the Marmara, basically it changes the whole response in the Marmara for that particular reason.

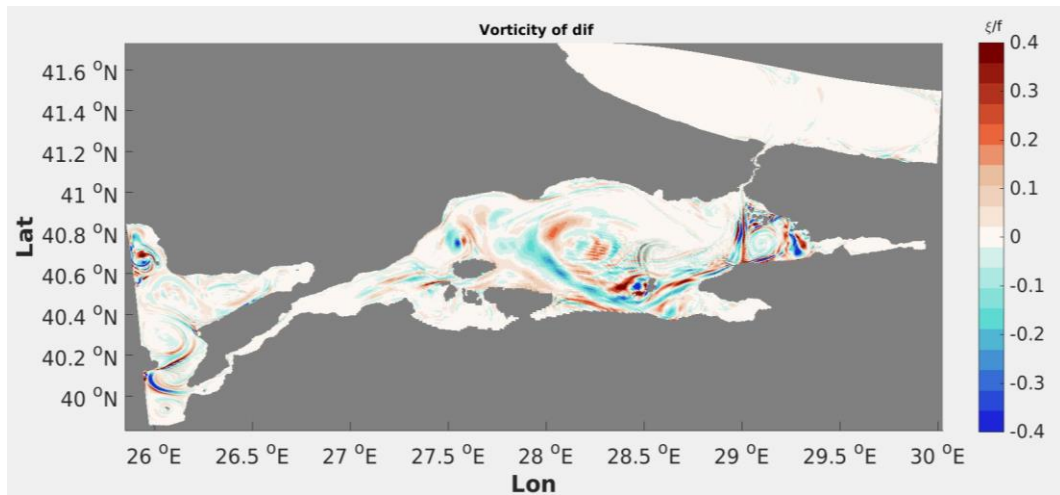


Figure 5.9 : Change Sea Surface Height Difference in the Marmara under the coupling behavior of Strait System.

In vorticity map, issued jet splits into three same as before but directed different than the hydrostatic model shown before. Main crucial outcome of this is in north-west of the Imrali island. Jet turns around southern side of the island and creates an upwelling close to the island. Bending of the jet trough the Southern side of the Marmara has an intense effect in the circulation pattern in the northern side of the Marmara island. Around the Marmara island, especially northern side of Avşa island, jet affect can be seen where the bending of the southern side of the jet go towards northern side of the Marmara Sea.

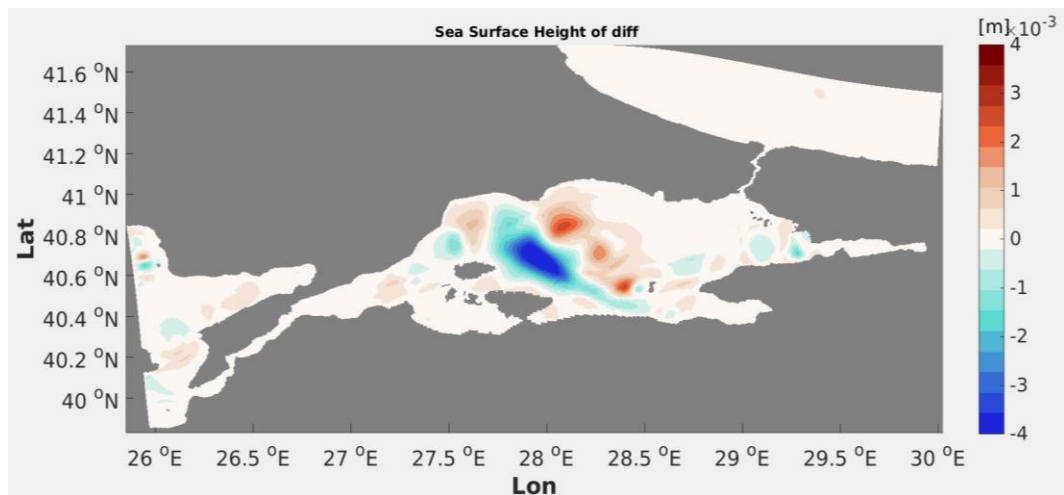


Figure 5.10 : Sea surface vorticity difference between two simulations.



6. CONCLUSIONS

In this thesis, 3-D numerical analyses of hydrodynamic behavior of TSS as an integrated coupled system under certain parametric conditions is studied. We performed two concurrent simulations which are using the same domain setup. In the first simulation (control case), hydrostatic approximation is made in the z-component of the momentum equation. We integrated the simulations over 33 days and analyzed flow fields including temperature and salinity averaged last five days of integration time. We found that three distinct water masses (i.e. Aegean Sea, Black Sea and the interfacial layer in between) successfully captured in the model. The vertical exchange between Aegean and Black Sea is evident at the Straits of Dardanelle and Bosphorus. The hydrostatic model findings are similar to those proposed by Sannino et al. (2017). For the non-hydrostatic model, we solve full vertical acceleration term equation instead of hydrostatic balance. The same modelling procedure as the control case is applied. Specifically, we aim to observe local effects on small-scale structures and turbulent effects of flow in the complex topography using a non-hydrostatic model. By taking the difference of these two simulations, we can investigate performance of non-hydrostatic model in terms of mixing and circulation compared to the standard hydrostatic model.

Although previous studies for TSS advised to employ non-hydrostatic model for the future, our study demonstrates the differences between two model simulations are minor. Therefore, we can conclude that, using a non-hydrostatic model, as presented here by using MITgcm based setup, does not gain significant improvements in terms of either temperature and salinity distribution or in the circulation pattern. We found that the salinity difference between two model along the thalweg is only 0.25 psu while the temperature difference is 2 degrees. The biggest difference between two models is on the surface circulation especially in the vorticity field. Location of the basin scale gyre and mesoscale eddies are different amongst the simulations. We should also emphasize that current horizontal resolution in the model might not be high enough to capture the necessary dynamical processes such as Kelvin-Helmholtz instabilities.



7. FUTURE STUDIES

As for future works, more realistic configuration of the MITgcm should be tested using proper wind and buoyancy forcing on the surface and lateral boundary conditions from reanalysis models for the Black and Aegean Seas. In addition to that, to resolve the real mixing scales more high resolution might be needed for the non-hydrostatic case. Due to our computational power, this was not feasible in this study. Finally, testing different vertical mixing schemes should be also area of active research especially representing the exchange flows in the Straits.



REFERENCES

- Adcroft, A., and Campin, J.-M.** (2004), Rescaled height coordinates for accurate representation of free-surface flows in ocean circulation models, *Ocean Modelling*, **7(3-4)**, 269-284.
- Aydođdu, A., Hoar, T. J., Vukicevic, T., Anderson, J. L., Pinardi, N., Karspeck, A., Hendricks, J., Collins, N., Macchia, F., and Özsoy, E.** (2018), OSSE for a sustainable marine observing network in the Sea of Marmara, *Nonlinear Processes in Geophysics*, **25(3)**, 537-551.
- Beji, S., and Battjes, J.** (1994), Numerical simulation of nonlinear wave propagation over a bar, *Coastal Engineering*, **23(1-2)**, 1-16.
- Beşiktepe Ş, Özsoy E, Latif MA, Oğuz T** (2000). Marmara Denizi'nin Hidrografisi ve Dolaşımı (Hydrography and Circulation of the Marmara Sea). In: Öztürk B et al. (eds) Marmara Sea 2000 Symposium Book. TÜDAV Publication, İstanbul, (in Turkish)
- Beşiktepe, Ş., Özsoy, E., and Ünlüata, Ü.** (1993), Filling of the Marmara Sea by the Dardanelles lower layer inflow, *Deep Sea Research Part I: Oceanographic Research Papers*, **40(9)**, 1815-1838.
- Beşiktepe, Ş. T., Sur, H. I., Özsoy, E., Latif, M. A., Oğuz, T., and Ünlüata, Ü.** (1994), The circulation and hydrography of the Marmara Sea, *Progress in Oceanography*, **34(4)**, 285-334.
- Bayazit, M. And Sümer, B. M.** (1982), *Oceanographie and hydraulic investigations of the Bosphrous. Vol.II. Final Report (TÜBİTAK), İTÜ, 23p.*
- Book, J. W., Jarosz, E., Chiggiato, J., and Beşiktepe, Ş.** (2014), The oceanic response of the Turkish Straits System to an extreme drop in atmospheric pressure, *Journal of Geophysical Research: Oceans*, **119(6)**, 3629-3644.
- Campin, J.-M., Adcroft, A., Hill, C., and Marshall, J.** (2004), Conservation of properties in a free-surface model, *Ocean Modelling*, **6(3-4)**, 221-244.
- Chiggiato, J., Jarosz, E., Book, J. W., Dykes, J., Torrisi, L., Poulain, P.-M., Gerin, R., Horstmann, J., and Beşiktepe, Ş.** (2012), Dynamics of the circulation in the Sea of Marmara: numerical modeling experiments and observations from the Turkish straits system experiment, *Ocean Dynamics*, **62(1)**, 139-159.
- Cushman-Roisin, B., and Beckers, J.-M.** (2011), *Introduction to geophysical fluid dynamics: physical and numerical aspects*, Academic press.
- Demyshev, S., and Dovgaya, S.** (2007), Numerical experiment aimed at modeling the hydrophysical fields in the Sea of Marmara with regard for Bosphorus and Dardanelles, *Physical Oceanography*, **17(3)**, 141-153.

- Demyshev, S., Dovgaya, S., and Ivanov, V.** (2012), Numerical modeling of the influence of exchange through the Bosphorus and Dardanelles Straits on the hydrophysical fields of the Marmara Sea, *Izvestiya, Atmospheric and Oceanic Physics*, **48(4)**, 418-426.
- Dorrell, R., Peakall, J., Sumner, E., Parsons, D., Darby, S., Wynn, R., Özsoy, E., and Tezcan, D.** (2016), Flow dynamics and mixing processes in hydraulic jump arrays: Implications for channel-lobe transition zones, *Marine Geology*, **381**, 181-193.
- Göktaşan, E., Tur, H., Ecevitöđlu, B., Görüm, T., Türker, A., Tok, B., Çađlak, F., Birkan, H., and Şimşek, M.** (2005), Evidence and implications of massive erosion along the Strait of İstanbul (Bosphorus), *Geo-Marine Letters*, **25(5)**, 324-342.
- Göktaşan, E., Ergin, M., Özyalvaç, M., Sur, H. İ., Tur, H., Görüm, T., Ustaömer, T., Batuk, F. G., Alp, H., and Birkan, H.** (2008), Factors controlling the morphological evolution of the Çanakkale Strait (Dardanelles, Turkey), *Geo-Marine Letters*, **28(2)**, 107-129.
- Gregg, M. C., and Özsoy, E.** (1999), Mixing on the Black Sea shelf north of the Bosphorus, *Geophysical Research Letters*, **26(13)**, 1869-1872.
- Gregg, M. C., and Özsoy, E.** (2002), Flow, water mass changes, and hydraulics in the Bosphorus, *Journal of Geophysical Research: Oceans*, **107(C3)**.
- Gurses, O., Aydođdu, A., Pınardı, N., and Özsoy, E.** (2016), A Finite Element Modeling Study of the Turkish Straits System, in *The Sea of Marmara Marine Biodiversity, Fisheries, Conservation and Governance*, edited, pp. 169-184, TUDAV.
- Horn, D., Imberger, J., and Ivey, G.** (2001), The degeneration of large-scale interfacial gravity waves in lakes, *Journal of Fluid Mechanics*, **434**, 181-207.
- Hundsdorfer, W., Koren, B., Van Loon, M., and Verwer, J.** (1995), A positive finite-difference advection scheme applied on locally re ned grids, *J. Comp. Phys*, **117**, 35-46.
- Ilıcak, M., and Armi, L.** (2010), Comparison between a non-hydrostatic numerical model and analytic theory for the two-layer exchange flows, *Ocean Modelling*, **35(3)**, 264-269.
- Ilıcak, M., Özgökmen, T. M., Özsoy, E., and Fischer, P. F.** (2009), Non-hydrostatic modeling of exchange flows across complex geometries, *Ocean Modelling*, **29(3)**, 159-175.
- Jackett, D. R., and Mcdougall, T. J.** (1995), Minimal adjustment of hydrographic profiles to achieve static stability, *Journal of Atmospheric and Oceanic Technology*, **12(2)**, 381-389.
- Jankowski, J. A.** (1999), A non-hydrostatic model for free surface flows, *Inst. für Strömungsmechanik und Elektronisches Rechnen im Bauwesen*.
- Jarosz, E., Teague, W. J., Book, J. W., and Beşiktepe, Ş.** (2011a), On flow variability in the Bosphorus Strait, *Journal of Geophysical Research: Oceans*, **116(C8)**.
- Jarosz, E., Teague, W. J., Book, J. W., and Beşiktepe, Ş.** (2011b), Observed volume fluxes in the Bosphorus Strait, *Geophysical Research Letters*, **38(21)**.
- Jarosz, E., Teague, W. J., Book, J. W., and Beşiktepe, Ş. T.** (2012), Observations on the characteristics of the exchange flow in the Dardanelles Strait, *Journal of Geophysical Research: Oceans*, **117(C11)**.

- Jarosz, E., Teague, W. J., Book, J. W., and Beşiktepe, Ş. T.** (2013), Observed volume fluxes and mixing in the Dardanelles Strait, *Journal of Geophysical Research: Oceans*, **118(10)**, 5007-5021.
- Kanarska, Y., and Maderich, V.** (2008), Modelling of seasonal exchange flows through the Dardanelles Strait, *Estuarine, Coastal and Shelf Science*, **79(3)**, 449-458.
- Marshall, J., Hill, C., Perelman, L., and Adcroft, A.** (1997a), Hydrostatic, quasi-hydrostatic, and nonhydrostatic ocean modeling, *Journal of Geophysical Research: Oceans*, **102(C3)**, 5733-5752.
- Marshall, J., Adcroft, A., Hill, C., Perelman, L., and Heisey, C.** (1997b), A finite-volume, incompressible Navier Stokes model for studies of the ocean on parallel computers, *Journal of Geophysical Research: Oceans*, **102(C3)**, 5753-5766.
- Marshall, J., and Schott, F.** (1999), Open-ocean convection: Observations, theory, and models, *Reviews of Geophysics*, **37(1)**, 1-64.
- Mellor, George L.** (1996). *Introduction to physical oceanography*. Springer. p. 169
- Moum, J., Farmer, D., Smyth, W., Armi, L., and Vagle, S.** (2003), Structure and generation of turbulence at interfaces strained by internal solitary waves propagating shoreward over the continental shelf, *Journal of Physical Oceanography*, **33(10)**, 2093-2112.
- Müller, W.-C., and Grappin, R.** (2005), Spectral energy dynamics in magnetohydrodynamic turbulence, *Physical Review Letters*, **95(11)**, 114502.
- Nash, J. D., and Moum, J. N.** (2005), River plumes as a source of large-amplitude internal waves in the coastal ocean, *Nature*, **437(7057)**, 400.
- Oguz, T.** (2005), Hydraulic adjustments of the Bosphorus exchange flow, *Geophysical research letters*, **32(6)**.
- Oguz, T., and Sur, H.** (1989), A 2-layer model of water exchange through the Dardanelles strait, *Oceanologica Acta*, **12(1)**, 23-31.
- Oguz, T., Özsoy, E., Latif, M. A., Sur, H. I., and Ünlüata, Ü.** (1990), Modeling of hydraulically controlled exchange flow in the Bosphorus Strait, *Journal of Physical Oceanography*, **20(7)**, 945-965.
- Ozsoy, E., Latif, M. A., Besiktepe, S., Cetin, N., Gregg, M. C., Belokopytov, V., Goryachkin, Y., and Diaconu, V.** (1998), The Bosphorus Strait: Exchange fluxes, currents and sea-level changes, *NATO Science Series 2 Environmental Security*, **47(2)**, 1-28.
- Özsoy, E., and Beşiktepe, Ş.** (1995), Sources of double diffusive convection and impacts on mixing in the Black Sea, *Double-Diffusive Convection*, 261-274.
- Özsoy, E., and Ünlüata, Ü.** (1997), Oceanography of the Black Sea: a review of some recent results, *Earth-Science Reviews*, **42(4)**, 231-272.
- Özsoy, E., Di Iorio, D., Gregg, M. C., and Backhaus, J. O.** (2001), Mixing in the Bosphorus Strait and the Black Sea continental shelf: observations and a model of the dense water outflow, *Journal of Marine Systems*, **31(1-3)**, 99-135.
- Pacanowski, R., and Philander, S.** (1981), Parameterization of vertical mixing in numerical models of tropical oceans, *Journal of Physical Oceanography*, **11(11)**, 1443-1451.

Sánchez-Garrido, J. C., Sannino, G., Liberti, L., García Lafuente, J., and Pratt, L. (2011), Numerical modeling of three-dimensional stratified tidal flow over Camarinal Sill, Strait of Gibraltar, *Journal of Geophysical Research: Oceans*, **116(C12)**.

Schroeder, K., García-Lafuente, J., Josey, S. A., Artale, V., Nardelli, B. B., Carrillo, A., Gačić, M., Gasparini, G. P., Herrmann, M., Lionello, P., Ludwig, W., Millot, C., Özsoy, E., Pisacane, G., Sánchez-Garrido, J. C., Sannino, G., Santoleri, R., Somot, S., Struglia, M., Stanev, E., Taupier-Letage, I., Tsimplis, M. N., Vargas-Yañez, M., Zervakis, V., G. Zodiatis (2012), Chapter 3: Circulation of the Mediterranean Sea and its Variability, In: Lionello, P. (ed.), *The Climate of the Mediterranean Region—From the past to the future*, Elsevier, 592 p

Sannino, G., Sözer, A., and Özsoy, E. (2017), A high-resolution modelling study of the Turkish Straits System, *Ocean Dynamics*, **67(3-4)**, 397-432.

Sannino, G., Garrido, J. S., Liberti, L., and Pratt, L. (2014), Exchange flow through the Strait of Gibraltar as simulated by a σ -coordinate hydrostatic model and a z-coordinate nonhydrostatic model, *The Mediterranean Sea: Temporal Variability and Spatial Patterns*, 25-50.

Seyir Hidrografi ve Oşinografi Dairesi Başkanlığı (2009). *Türk Boğazlar Atlası*. Cubuklu, Istanbul: Seyir Hidrografi ve Osinografi Dairesi Başkanlığı Yayını.

Schroeder, K., García-Lafuente, J., Josey, S. A., Artale, V., Nardelli, B. B., Carrillo, A., Gačić, M., Gasparini, G. P., Herrmann, M., and Lionello, P. (2012), Circulation of the Mediterranean Sea and its variability, in *The climate of the Mediterranean region*, edited, pp. 187-256, Elsevier.

Sözer, A. (2013), Numerical modeling of the Bosphorus exchange flow dynamics, Ph. D. thesis, Institute of Marine Sciences, Middle East Technical University, Erdemli, Mersin, Turkey.

Sözer, A., and Özsoy, E. (2002), A three-dimensional model of Bosphorus Strait dynamics, paper presented at The 2nd Meeting on the Physical Oceanography of Sea Straits, Villefranche, 15th-19th.

Sözer, A., and Özsoy, E. (2017), Modeling of the Bosphorus exchange flow dynamics, *Ocean dynamics*, **67(3-4)**, 321-343.

Stanev, E. V., Grashorn, S., and Zhang, Y. J. (2017), Cascading ocean basins: numerical simulations of the circulation and interbasin exchange in the Azov-Black-Marmara-Mediterranean Seas system, *Ocean Dynamics*, **67(8)**, 1003-1025.

Stashchuk, N., and Hutter, K. (2001), Modelling of water exchange through the Strait of the Dardanelles, *Continental Shelf Research*, **21(13-14)**, 1361-1382.

Stewart, R. H. (2008), *Introduction to physical oceanography*, Robert H. Stewart.

Ünlülata, Ü., Oğuz, T., Latif, M., and Özsoy, E. (1990), On the physical oceanography of the Turkish Straits, in *The physical oceanography of sea straits*, edited, pp. 25-60, Springer.

CURRICULUM VITAE

Name Surname : Ece Nil Parkan
Place and Date of Birth : Istanbul / 15.09.1991
E-Mail : nilparkan@hotmail.com

EDUCATION :

- **B.Sc.** : 2012, Istanbul Technical University, Faculty of Mines, Geophysical Engineering
- **M.Sc.** : 2018, Istanbul Technical University, Eurasia Earth Sciences, Geodynamics Program